Revisiting anomalous structures in liquid Ga

K. H. Tsai, Ten-Ming Wu, and Shiow-Fon Tsay

Citation: The Journal of Chemical Physics **132**, 034502 (2010); doi: 10.1063/1.3294565
View online: http://dx.doi.org/10.1063/1.3294565
View Table of Contents: http://scitation.aip.org/content/aip/journal/jcp/132/3?ver=pdfcov
Published by the AIP Publishing

Revisiting anomalous structures in liquid Ga

K. H. Tsai,[1] Ten-Ming Wu,[1,a)] and Shiow-Fon Tsay[2]
[1]*Institute of Physics, National Chiao-Tung University, HsinChu, Taiwan 300, Republic of China*
[2]*Department of Physics, National Sun Yat-sen University, Kaohsiung, Taiwan 804, Republic of China*

(Received 2 November 2009; accepted 29 December 2009; published online 20 January 2010)

In terms of an interatomic pair potential, which well characterizes the dynamic properties of liquid Ga, we investigate again the origin of the well known high-q shoulder in the static structure factor of the liquid. Similar to the results of Gong's simulation at high temperature, dimers with extremely short bond lengths are indeed found in our model just above the melting point, but our results indicate that it is unlikely for the high-q shoulder to be produced by these dimers. Instead, based on our model, the high-q shoulder is resulted from some medium-range order, which is related to the structures beyond the first shell of the radial distribution function, caused by Friedel oscillations within a nanoscale range. © *2010 American Institute of Physics*. [doi:10.1063/1.3294565]

I. INTRODUCTION

Polyvalent liquid metals (Ga, Si, Ge, Sn, As, Sb, and Bi) are well known for anomalous structures, mainly characterized by a shoulder appearing on the high-q side of the first peak in the static structure factors of these liquids.[1,2] The origin of the shoulder structures has been a long-standing subtle problem in liquid metal physics and several scenarios have been proposed.[3–9] Using the interatomic pair potentials derived from the pseudopotential theory, which generally have a ledge-shaped repulsive core and the long-ranged Friedel oscillations, Hafner and co-workers reproduced the shoulder structures in liquid Ga, Ge, and Si,[5] and concluded that the peculiar static structure factor is determined by two characteristic lengths: the effective hard-sphere diameter required by sphere packing and the Friedel wavelength λ_F associated with the oscillatory part of the pair potential. The high-q shoulder is, therefore, predicted to occur near $2\pi/\lambda_F$.

Among these polyvalent elements, Ga shows uncommon properties, including low melting temperature (T_m=302 K), an increase in density upon melting, and complex solid-state phases under high pressure.[10] These properties are closely related to the existence of the covalent dimers, with a bond length of 2.44 Å, in solid Ga(α-Ga) at the ambient pressure.[11] Based on an *ab initio* simulation of Ga at T=1000 K, Gong *et al.*[7] found the existence of very short-lived covalent dimers, which were considered as the remnants as α-Ga melts and expected to increase in concentration at lower temperatures. They attributed the high-q shoulder in the static structure factor above T_m to the presence of these covalent dimers.

By classical molecular dynamics (MD) simulations with an interatomic pair potential generated by a first-principles pseudopotential theory, Tsay[12] reproduced not only the shoulder structures of liquid Ga, but also the naive structural variation in Ga as rapidly quenched from the liquid state to the supercooled and glassy states and then reheated. After analyzing the liquid and amorphous structures, Tsay[8] postulated that the shoulder structures in liquid Ga are primarily due to some four-atom clusters, which become predominated in the amorphous states and β-crystal. Thus, the origin of the high-q shoulder in the static structure factor of liquid Ga is still unclear and debated so far.

In the past decade, dynamics of liquid Ga has been intensively studied by inelastic scattering experiments.[13–17] The results of these experiments also provide information related to the structures of liquid Ga and play a role on examining the existing potential models used in simulations for mimicking the liquid. In Sec. II, we first investigate the validity of the pair potential $\phi(r)$ used in the simulations of Tsay by comparing the calculated dynamic quantities with several sets of inelastic scattering data, which include the dynamical structure factor $S(q,\omega)$, the dispersion relation, and the damping factor of collective excitations at low q as well as the linewidth of $S(q,\omega)$ at high q. Our results indicate that the model of Tsay, without any fitting parameters, is appropriate for describing the dynamics of liquid Ga. In Sec. III, we turn our attention to the structures produced by simulations with $\phi(r)$ at thermodynamic conditions of Ga at T =323 K. Dimers with bond lengths near 2.44 Å are indeed found in our simulation; however, we give several reasons to question the interpretation that the high-q shoulder in the static structure factor of liquid Ga is produced by the dimers themselves. On the other hand, by comparing the liquid structures generated with $\phi(r)$ truncated at different distances at the same NVT conditions, we find that the high-q shoulder is associated with some medium-range order, which is related to the structures beyond the first shell around a partilce.[18] The medium-range order, caused by the Friedel oscillations within a range of nanoscale, favors the formation of the four-atom clusters pointed out by Tsay. Our conclusions are given in Sec. IV.

II. COMPARISON OF OUR MODEL WITH THE EXPERIMENTAL RESULTS

Generated by the generalized energy independent nonlocal model pseudopotential (GEINMP) theory,[8] the inter-

a)Author to whom correspondence should be addressed. Electronic mail: tmw@faculty.nctu.edu.tw.

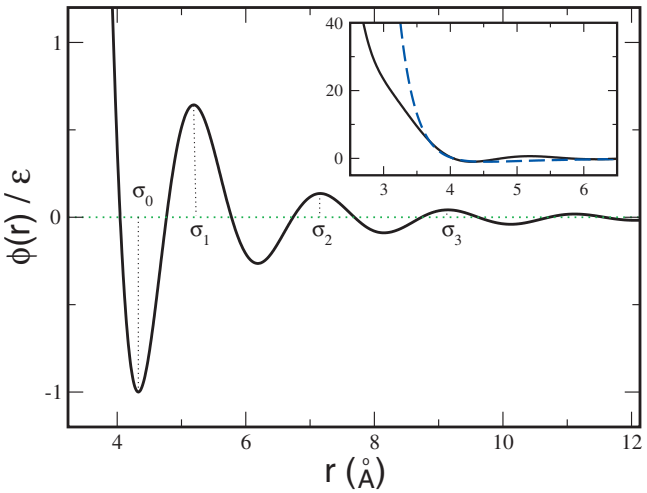

FIG. 1. Interatomic pair potential $\phi(r)$. ε is the depth of the first attractive well, corresponding to a temperature about 47 K. σ_0 is the location of the first minimum of $\phi(r)$. σ_1, σ_2, and σ_3 are the locations of the first, second, and third maxima of the oscillatory part, respectively. The inset shows the comparison between $\phi(r)$ (solid line) and the LJ potential (dashed line) with the same ε and the distance at the first zero of the potential.

atomic pair potential $\phi(r)$, shown in Fig. 1, has a soft repulsive core and an oscillatory part. In the oscillatory part, which has λ_F=1.93 Å, the minimum of the first attractive well is located at σ_0=4.32 Å, and the first, second, and third maxima of $\phi(r)$ are located at σ_1=5.17 Å, σ_2=7.15 Å, and σ_3=9.13 Å, respectively.

As with our previous works,[19,20] we perform MD simulations of 3500 particles interacting with $\phi(r)$ at T=323 K and number density ρ=0.05 Å^{-3}, which is close to the ion density of liquid Ga at this temperature and pressure of about 1 bar. In our simulation, the predictor-corrector algorithm is used and a time step is 5.45 fs. Under the periodic boundary conditions, particles are confined in a cubic box of length 41.25 Å and $\phi(r)$ is terminated at half of the box size.

Relative to $\phi(r)$, the first and second peaks of the radial distribution function $g(r)$ of the simulated liquid are located at 2.77 and 5.46 Å, which are distances well inside the repulsive core of $\phi(r)$ and slightly over the first maximum of Friedel oscillations, respectively. The calculated static structure factor $S(q)$, shown in Fig. 4, has the main peak at q_M =25.4 nm^{-1}, followed by a shoulder around 32.5 nm^{-1}, which exactly equals $2\pi/\lambda_F$.

In the following, we compare the dynamic properties calculated by the model of $\phi(r)$ to the experimental data.

A. Dynamic structure factors at low *q*

The dynamic structure factor $S_{\mathrm{MD}}(q,\omega)$ of $\phi(r)$ is obtained via a time Fourier transform of the intermediate scattering function generated by our simulation.[19] To compare to the experimental data of inelastic x-ray scattering (IXS), $S_{\mathrm{MD}}(q,\omega)$ is weighted by the detailed balance factor and then convoluted with the instrument resolution function, which has a width of 3.0 meV, used in the experiment.[13] The comparisons of our results with the experimental data of liquid Ga at T=315 K for three wave vectors are presented in Fig. 2, in which no fitting parameter is involved. Our model generally describes the dynamic structure factor of liquid Ga, except for a slight deviation at q=5.75 nm^{-1} due to the system size of our simulation.

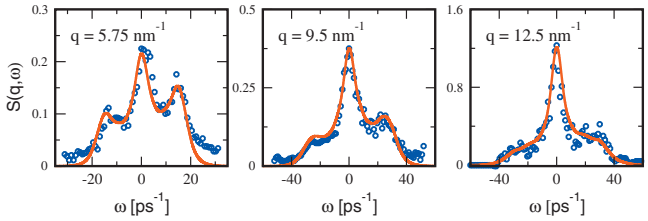

FIG. 2. Dynamic structure factor of liquid Ga. The solid lines are the results calculated by our model at T=323 K and the circles are the IXS data at T=315 K (Ref. 13).

B. Sound speed and the damping factor of collective excitations

Shown in Fig. 3 is the longitudinal current spectra $C_L(q,\omega)$ calculated by our model and analyzed with a damped harmonic oscillator (DHO) model,[21] which is expressed as

$$C_L(q,\omega) = \frac{A_q \omega_q \Gamma_q \omega}{(\omega^2 - \omega_q^2)^2 + (\Gamma_q \omega)^2}, \tag{1}$$

where the fitting parameters A_q, ω_q, and Γ_q are referred to the amplitude, energy, and damping of the longitudinal excitations at q, respectively. Obtained from the fits, ω_q and Γ_q at small q are found to be linear with q. In the insets of Fig. 3, the fit results of the dispersion relation and the damping fac-

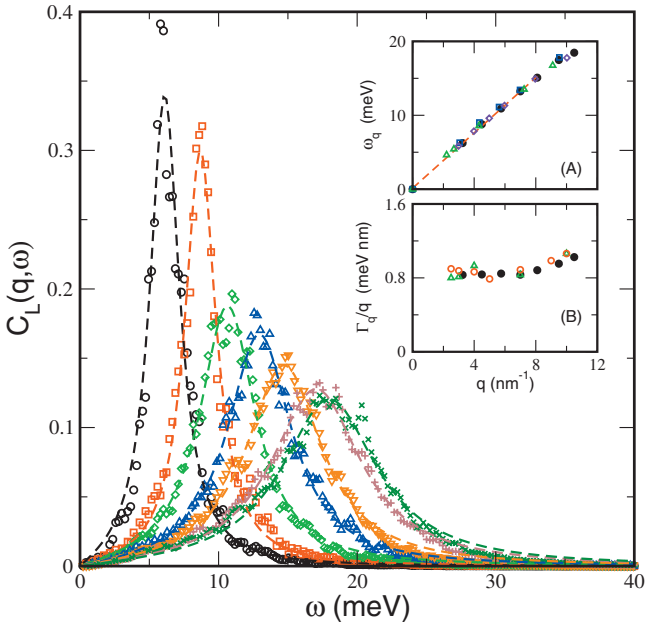

FIG. 3. Longitudinal current spectra $C_L(q,\omega)$ of our model at q =3.25 nm^{-1} (circles), 4.5 nm^{-1} (squares), 5.75 nm^{-1} (diamonds), 7.0 nm^{-1} (up triangles), 8.1 nm^{-1} (down triangles), 9.5 nm^{-1} (pluses), and 10.5 nm^{-1} (crosses). The dashed lines are the fits with the DHO model given in the text. The insets show (a) the excitation energy ω_q and (b) the damping factor Γ_q/q. The filled circles in (a) and (b) are the fit results of our model. In (a), the dashed line is the sound dispersion, and the open squares and diamonds are two sets of the IXS data at T=315 K (Ref. 13) and T=373 K (Ref. 17), respectively. The open triangles in (a) and (b) are the INS data at T =320 K and the open circles in (b) are the results of other model (Ref. 14).

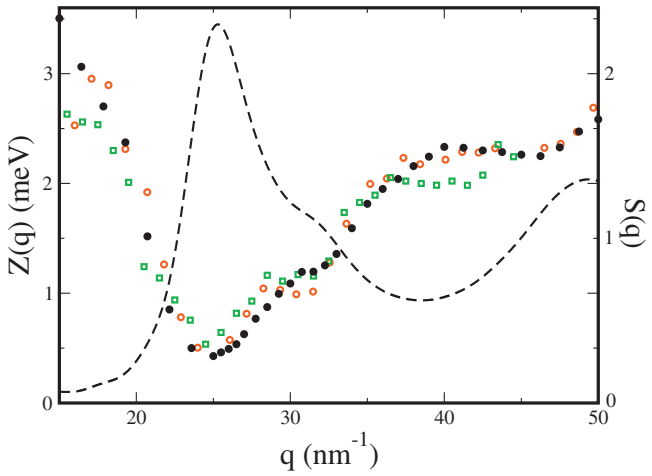

FIG. 4. Spectral linewidth $Z(q)$ of dynamic structure factor at high q. The filled circles are the results of our model. The open circles and squares are the data of IXS (Ref. 15) and QENS (Ref. 16) at $T=315$ K, respectively. The dashed line is the $S(q)$ of our model with a scale referred to the right axis.

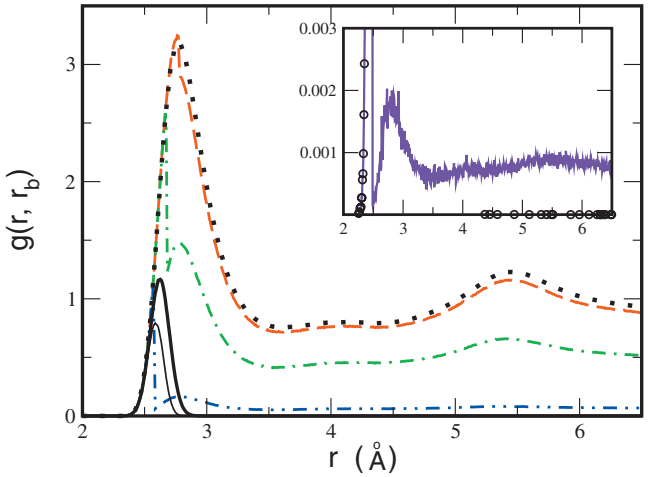

FIG. 5. Radial distribution functions of bonded atoms for $r_b=2.78$ Å (dashed line), 2.68 Å (dotted-dashed line), and 2.58 Å (dotted-dotted-dashed line) in the main panel and for $r_b=2.48$ Å (solid line) and 2.38 Å (open circles) in the inset. The dotted line is $g(r)$ of the liquid. The thick and thinner solid lines are the distributions of the NN and the MNN pairs in the liquid, respectively (Ref. 25).

tor Γ_q/q versus q are compared to the corresponding experimental data.[13,14,17] Through the low-q limit of the dispersion relation, the sound speed of our model is estimated to be 2860 cm/s, which is consistent with the adiabatic sound speed of liquid Ga just above T_m.[22] Also, the damping factor Γ_q/q of our model is in good agreement with those obtained by inelastic neutron scattering (INS) and the prediction of other model.[14]

C. Spectral linewidth of dynamic structure factor at high *q*

For the wave vectors in the kinetic regime, the sound waves in a liquid are strongly damped and the dynamic structure factor has only a single, Lorentzian-like central peak.[23] For q larger than 15 nm^{-1}, $S_{\mathrm{MD}}(q,\omega)$ of our model can be fitted with a single Lorentzian. Shown in Fig. 4, the linewidth of the fit Lorentzian $Z(q)$ as a function of q exhibits a minimum, which is the so-called de Gennes narrowing, very close to q_M.[24] In the experimental data of the spectral linewidth of dynamic structure factor, an anomaly is observed on the high-q side of the de Gennes narrowing; the anomaly is a second minimum by the IXS technique[15] but a shoulder by the quasielastic neutron scattering (QENS) technique.[16] In our data of $Z(q)$, we also observe a shoulder on the high-q side of the de Gennes narrowing. The shoulder in $Z(q)$ is almost at the same position of the high-q shoulder in $S(q)$, with the width of the shoulder somewhat narrower than the one observed in the QENS experiment.

According to the comparisons given above, we confirm that our model is appropriate for describing the structures and dynamic properties of liquid Ga just above T_m.

III. ORIGIN OF THE ANOMALOUS STRUCTURES

A. Are the anomalous structures due to the dimers?

In order to address whether the shoulder appearing in $S(q)$ of our model arises from the dimers as proposed by Gong *et al.*,[7] we defined the bonded atoms as those having at least one neighbor within a cutoff r_b. From the distribution of the nearest-neighbor (NN) pairs shown in Fig. 5, we find that the values of r_b for our model is roughly from 2.34 to 2.93 Å. Besides the atomic pairs with separations less than r_b, which are referred to dimers, the radial distribution function $g(r,r_b)$ of the bonded atoms also has contributions from the interdimer pairs which separations are larger than r_b.

At $r_b=2.38$ Å, as shown in Fig. 5, the contributions to $g(r,r_b)$ from these two kinds of atomic pairs are well separated because the bonded atoms are rare. The concentration of the dimers is quite low; in average, only one dimer is found in each configuration of 3500 particles. The dimers with such a short bond length are actually the mutual NN (MNN) pairs, which are two atoms with each other as NNs.[25] Due to their short separations, the repulsive interaction within each MNN pair is much stronger than those felt by other atomic pairs in the liquid and this strong repulsion makes the MNN pair survive only within a very short lifetime (less than 100 fs) during a collision. As r_b increases, the dimers are not necessarily the MNN pairs and some dimers are connected to form clusters, with a result on $g(r,r_b)$ that the distribution is no longer separated but has a sharp jump at r_b and the interdimer contribution generally reflects the behavior of $g(r)$. At $r_b=2.78$ Å, the similarity between $g(r,r_b)$ and $g(r)$ indicates that almost all of atoms in the simulation are the bonded atoms.

The structure factor $S(q,r_b)$ of the bonded atoms with a cutoff at r_b can be obtained via the formula

$$S(q,r_b)=1+4\pi\rho\int_0^\infty (g(r,r_b)-n_b)\frac{\sin(qr)}{qr}r^2dr, \qquad (2)$$

where $n_b=N_b/N$ is the percentage of the bonded atoms in the simulated system. Correspondingly, $S(q,r_b)$ can be separated into $S_d(q,r_b)$ and $\Delta S(q,r_b)$, which are the structure factor due to the dimers and the residue owing to the interdimer pairs, respectively.

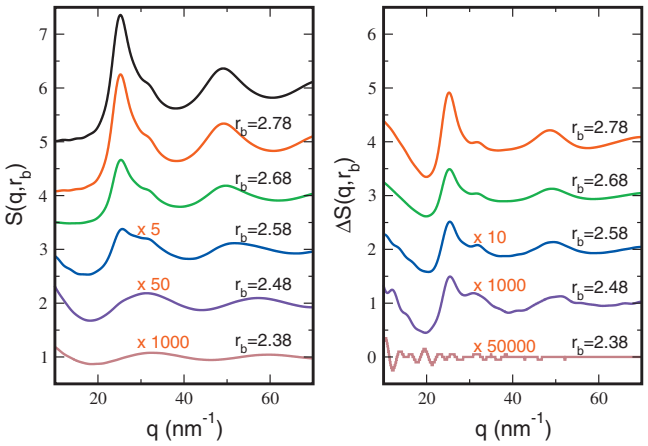

FIG. 6. Bonded-atoms structure factors $S(q,r_b)$ (left panel) and the residual structure factors $\Delta S(q,r_b)$ (right panel) for the r_b values in angstrom. Each curve is shifted upward by one unit from its lowered one. The top one in the left panel is $S(q)$ of the liquid. The values of the curves indicated with a red number have been amplified by the number.

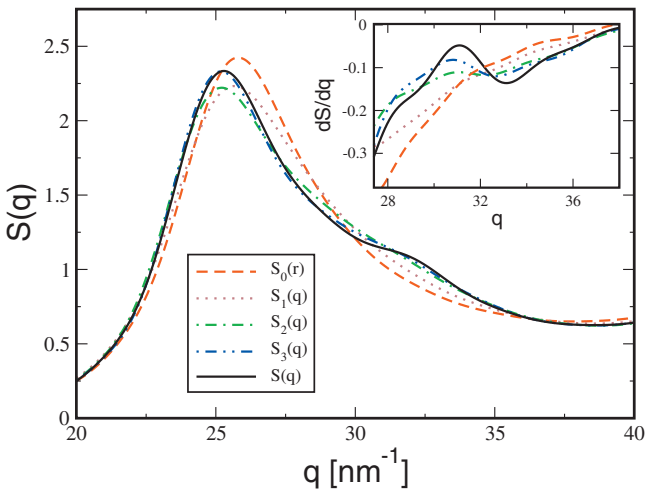

FIG. 7. Variation in static structure factor with the interaction range of $\phi(r)$. The solid line is for $S(q)$ of $\phi(r)$ and the dashed line is for $S_0(q)$ of $\phi_0(r)$ truncated at 4.32 Å. The dotted, dotted-dashed, and dotted-dotted-dashed lines are for $S_i(q)$ of $\phi_i(r)$ $(i=1,2,3)$, truncated at 5.17, 7.15, and 9.13 Å, respectively. The inset shows the first derivative of the corresponding static structure factors with respect to q.

$S(q,r_b)$ and $\Delta S(q,r_b)$ of our model are presented in Fig. 6 for several values of r_b. At $r_b=2.38$ Å, $S(q,r_b)$ is almost equivalent to $S_d(q,r_b)$ which oscillations can be approximated as $\sin(qr_b)/qr_b$.[24] As r_b increases, the behavior of $S(q,r_b)$ changes from the dimer structure factor to $S(q)$ of the liquid, with the main peak of $S(q)$ developing from a peak not appearing in $S_d(q,r_b)$ and the location of the high-q shoulder in $S(q)$ close to the maximum of $S_d(q,r_b)$ around $q\approx 32$ nm^{-1}. The variation in $S(q,r_b)$ with r_b agrees with Gong's results obtained by *ab initio* simulation at high temperature. However, the variations in $S_d(q,r_b)$ and $\Delta S(q,r_b)$ with r_b provide an evidence against the interpretation that the high-q shoulder originates from the dimers.

By increasing r_b up to 2.78 Å, $S_d(q,r_b)$ always behaves similarly, without much change in the oscillation but with a little increase in amplitude for more dimers are involved. On the contrary, the variation in $\Delta S(q,r_b)$ is quite dramatic. At $r_b=2.38$ Å, $\Delta S(q,r_b)$ is extremely small and fluctuated, since the interdimer pairs among the bonded atoms are rather rare. As r_b equals 2.48 Å, two peaks, with their positions very close to those of the main peak and the shoulder in $S(q)$, emerge in $\Delta S(q,r_b)$. By increasing r_b further, the two peaks are enhanced in value but their positions almost persist, and finally the shape of the two peaks is akin to the main peak and the shoulder in $S(q)$. This result gives an evidence that the high-q shoulder in $S(q)$ is associated with the interdimer pairs, rather than the dimers.

B. Medium-range order due to Friedel oscillations

To investigate the effective range of $\phi(r)$ to produce the shoulder in $S(q)$, we examine the variation in liquid structures with the interaction range of $\phi(r)$ from the repulsive core only to the full range. We have performed MD simulations at the same *NVT* conditions with the truncated pair potential $\phi_i(r)$ for $i=0,1,2,3$, which is obtained by truncating $\phi(r)$ at σ_i and shifting in energy by the value $\phi(\sigma_i)$ so that $\phi_i(r)$ has a finite range.[26] $\phi_0(r)$ is the repulsive core of $\phi(r)$. $\phi_1(r)$ contains the repulsive core and the first attractive well, with a depth corresponding to a temperature about 47 K. The ranges of $\phi_2(r)$ and $\phi_3(r)$ extend to include the first two and three attractive wells, respectively; the depths of these attractive wells decrease with increasing distance, as shown in Fig. 1. In the following, we present the static structure factors, the radial distribution functions and atomic bonded pairs (ABPs) (Ref. 8) of the fluids with the truncated $\phi_i(r)$.

1. Static structure factor

The static structure factors $S_i(q)$ of the fluids with $\phi_i(r)$ $(i=0,1,2,3)$ are shown in Fig. 7. $S_0(q)$ of the fluid with the repulsive core only is generally recovered back to the behavior of a hard-sphere fluid, with the first peak shifting to 25.7 nm^{-1} and increasing in magnitude. The essential difference between $S_0(q)$ and $S(q)$ is that there is no shoulder appearing on the high-q side of the first peak. By including the first attractive well in the pair potential, the first peak of $S_1(q)$, compared to $S_0(q)$, is lowered but has no significant change in position, while the values of $S_1(q)$ for q in the shoulder region, which is between 28 and 35 nm^{-1}, are elevated. The consequences of including the second attractive well are that the first peak of $S_2(q)$ shifts closer to that of $S(q)$ but has no change in magnitude and the values of $S_2(q)$ in the shoulder region are continuously elevated. The effect of extending the interaction range to include the third attractive well causes an increase in magnitude of the first peak and the appearance of a noticeable shoulder on the high-q side of the first peak; hence, $S_3(q)$ has a close resemblance to $S(q)$.

The appearance of the shoulder in the high-q region can be further identified by the derivative of $S_i(q)$ with respect to q, $dS_i(q)/dq$, which is shown in the inset of Fig. 7. In general, $dS_i(q)/dq$ on the high-q side of the first peak is negative and increases with q. A monotonic increase in $dS_i(q)/dq$ with q indicates that no shoulder appears in this region. Once a shoulder appears in $S_i(q)$, the behavior of $dS_i(q)/dq$ is

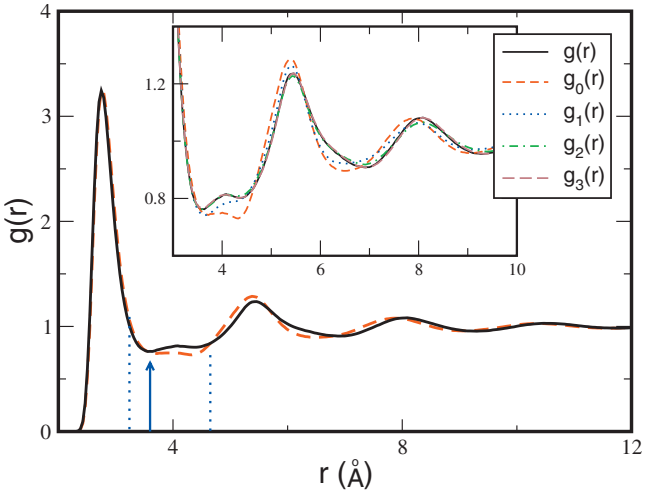

FIG. 8. Radial distribution functions of the liquid with $\phi(r)$ (solid line) and the fluid with $\phi_0(r)$ (dashed line). The two dashed lines indicate the distances of r_1 and r_2 in our evaluation for ΔN and the arrow indicates the bond length in the calculation of ABPs. The inset shows the variation in the second and third shells of the radial distribution function with the interaction range of $\phi(r)$.

distorted from a monotonic increase to the appearance of some extrema, where the slope of $dS_i(q)/dq$ is zero. The monotonic increase in $dS_0(q)/dq$ and $dS_1(q)/dq$ indicate that no shoulder appears in $S_0(q)$ or $S_1(q)$. $dS_2(q)/dq$ shows very weak extrema, signaling the emergence of a weak shoulder in $S_2(q)$. Evidenced by the clearly observed extrema in $dS_3(q)/dq$, the structures in the liquid of $\phi_3(r)$ are developed well enough to produce a shoulder in $S_3(q)$.

According to the results presented above, we conclude that the effective range of $\phi(r)$ for the full appearance of the shoulder structures should extend up to include the third attractive well; the effective range is, therefore, in a nanoscale.

2. Radial distribution function

In real space, the changes in the liquid structures with the range of pair potential are manifested in Fig. 8, which shows the comparison between $g(r)$ and the radial distribution functions $g_i(r)$ of the truncated $\phi_i(r)$. Clearly, all radial distribution functions possess almost the same first shell, indicating that dimers with extremely short bond lengths can be also found in the fluid with the repulsive core $\phi_0(r)$. Between the first and second peaks, all distribution functions have a small hump near 4 Å, which is close to the minimum of the first attractive well in $\phi(r)$. This small hump is also observed in the radial distribution function of liquid Ge.[27,28] In agreement with the case in static structure factor, the effective range in Friedel oscillations to make $g_i(r)$ saturated to $g(r)$ should include the first three attractive wells. As shown in the inset of Fig. 8, Friedel oscillations cause two effects on $g(r)$: pulling inward half a particle from the second shell to increase the small hump near 4 Å and pushing the second shell and the rest outward for compensation.[29] This gives an evidence that the high-q shoulder in $S(q)$ is associated with the structures beyond the first shell of $g(r)$, which possess some medium-range order in the liquid.[18]

3. Atomic bonded pairs

To manifest further the medium-range order due to Friedel oscillations, we calculate the averaged fractions of ABPs (Ref. 30) in the simulated liquids. It has been shown that as the system simulated with the pair potential generated by the GEINMP theory is quenched from liquid phase into amorphous solids or β crystal, the 1201-type ABPs become predominated. The 1201-type ABPs are clusters of four atoms, with two being a root pair and the other two being the common neighbors of the root pair within a bond length but the separation between the two common neighbors larger than the bond length.[12] Also, it is found that some large clusters formed with more 1201-type ABPs may produce a high-q shoulder in $S(q)$.[8] In this paper, we set the bond length to be 3.4 Å, which is close to the first-minimum distance of $g(r)$, so that the separation between the two common neighbors in the 1201-type ABPs is generally in the region of the small hump in $g(r)$. By comparing the calculated data given in Table I for the liquid of $\phi(r)$ and the fluid of $\phi_0(r)$, Friedel oscillations make the fraction of the 1201-type ABPs increase about 20%, which favor the occurrence of the high-q shoulder pointed out by Tsay.[8]

IV. CONCLUSIONS

In this paper, by classical MD simulation with an interatomic pair potential generated from the first-principles theory, we have reproduced the structural and dynamic properties of liquid Ga just above the melting temperature. Good agreement between the predictions of our model on dynamic properties and the experimental data suggests that our model is an appropriate one for describing liquid Ga.

Similar to the results of *ab initio* simulation reported by Gong *et al.*,[7] dimers with bond lengths comparable to that of the covalent molecules in solid α-Ga are indeed found in our model. However, we give several reasons to question the interpretation that the dimers are the origin of the high-q shoulder in the static structure factor of liquid Ga. First, the concentration of the dimers at temperatures just above melt-

TABLE I. Averaged fractions of ABPs N_{ijkl} in the fluids simulated with the full-range $\phi(r)$ and the truncated $\phi_i(r)$.

Pair potential	N_{1201}	N_{1211}	N_{1301}	N_{1311}	N_{1321}	N_{1421}	N_{1422}	N_{1431}
$\phi_0(r)$	0.156	0.048	0.114	0.253	0.067	0.052	0.105	0.081
$\phi_1(r)$	0.176	0.046	0.124	0.255	0.063	0.047	0.096	0.072
$\phi_2(r)$	0.191	0.046	0.133	0.252	0.059	0.042	0.091	0.064
$\phi_3(r)$	0.190	0.045	0.135	0.251	0.059	0.042	0.092	0.064
$\phi(r)$	0.188	0.045	0.134	0.251	0.059	0.042	0.093	0.065

ing point is quite low. Second, the extremely strong repulsion within a dimer makes the dimer unstable, surviving only for a very short lifetime during a collision. Besides these two, we provide evidences that the high-q shoulder is associated with the atomic pairs between the dimers, rather than the dimers themselves.

Our simulations indicate that Friedel oscillations produce a modulation on the local structures of particles, which are mainly determined by the soft repulsive core in our model. The modulation on the local structures gives rise to some stable medium-range order, which is related to the structures beyond the first shell of the radial distribution function. The high-q shoulder in the static structure factor is found to be associated with the medium-range order caused by Friedel oscillations. According to our model, the effective range of Friedel oscillations to produce the medium-range order should include, at least, the first three attractive wells, so that the effective range is in a nanoscale. Thus, our results are consistent with the picture given by Hafner *et al.*[5] that the shoulder structures are a result of the interplay between two length scales, characterizing the size of the repulsive core and the wavelength of Friedel oscillations.

The high-q shoulder in the static structure factor is a common feature to many polyvalent liquid metals. According to our study, the anomalous structures characterizing the high-q shoulder are quite complex, since a number of atoms, more than 20 estimated for liquid Ga, are involved. To manifest the anomalous structures, a picture of atomic structures in three-dimensional space is requested. This is challenging but important to fully understand the origin for the high-q shoulder of those polyvalent liquid metals and will be a future work.

ACKNOWLEDGMENTS

T. M. Wu and S. F. Tsay are indebted to the National Science Council of Taiwan, Republic of China for support under Grant No. NSC 97-2112-M-009-005-MY2 and NSC 98-2112-M-110-004-MY3, respectively.

[1] Y. Waseda, *The Structure of Non-Crystalline Materials, Liquids and Amorphous Solids* (McGraw-Hill, New York, 1980).
[2] J. Hafner, *From Hamiltonians to Phase Diagrams* (Springer-Verlag, Berlin, 1987).
[3] M. Silbert and W. H. Young, Phys. Lett. A **58**, 469 (1976).
[4] K. K. Mon, N. W. Ashcroft, and G. V. Chester, Phys. Rev. B **19**, 5103 (1979).
[5] J. Hafner and G. Kahl, J. Phys. F: Met. Phys. **14**, 2259 (1984).
[6] J. Hafner and W. Jank, Phys. Rev. B **42**, 11530 (1990).
[7] X. G. Gong, G. L. Chiarotti, M. Parrinello, and E. Tosatti, Europhys. Lett. **21**, 469 (1993).
[8] S. F. Tsay and S. Wang, Phys. Rev. B **50**, 108 (1994).
[9] L. E. Gonzalez, D. J. Gonzalez, and M. Silbert, Mol. Phys. **99**, 875 (2001).
[10] O. Degtyareva, M. I. McMahon, D. R. Allan, and R. J. Nelmes, Phys. Rev. Lett. **93**, 205502 (2004).
[11] X. G. Gong, G. L. Chiarotti, M. Parrinello, and E. Tosatti, Phys. Rev. B **43**, 14277 (1991).
[12] S. F. Tsay, Phys. Rev. B **50**, 103 (1994).
[13] T. Scopigno, A. Filipponi, M. Krisch, G. Monaco, G. Ruocco, and F. Sette, Phys. Rev. Lett. **89**, 255506 (2002).
[14] L. E. Bove, F. Formisano, F. Sacchetti, C. Petrillo, A. Ivanov, B. Dorner, and F. Barocchi, Phys. Rev. B **71**, 014207 (2005).
[15] T. Scopigno, R. Di Leonardo, L. Comez, A. Q. R. Baron, D. Fioretto, and G. Ruocco, Phys. Rev. Lett. **94**, 155301 (2005).
[16] F. J. Bermejo, I. Bustinduy, S. J. Levett, J. W. Taylor, R. Fernández-Perea, and C. Cabrillo, Phys. Rev. B **72**, 104103 (2005).
[17] S. Hosokawa, W. C. Pilgrim, H. Sinn, and E. E. Alp, J. Phys.: Condens. Matter **20**, 114107 (2008).
[18] S. R. Elliott, *Physics of Amorphous Materials*, 2nd ed. (Longman, Harlow, 1990).
[19] K. H. Tsai, T. M. Wu, S. F. Tsay, and T. J. Yang, J. Phys.: Condens. Matter **19**, 205141 (2007).
[20] K. H. Tsai and T. M. Wu, J. Chem. Phys. **129**, 024503 (2008).
[21] M. C. C. Ribeiro, M. Wilson, and P. A. Madden, J. Chem. Phys. **108**, 9027 (1998).
[22] M. Inui, S. Takeda, and T. Uechi, J. Phys. Soc. Jpn. **61**, 3203 (1992).
[23] T. Scopigno, G. Ruocco, and F. Sette, Rev. Mod. Phys. **77**, 881 (2005).
[24] J. P. Hansen and I. R. McDonald, *Theory of Simple Liquids* (Academic, New York, 2006).
[25] R. E. Larsen and R. M. Stratt, Chem. Phys. Lett. **297**, 211 (1998).
[26] N. Matsuda, K. Hoshino, and M. Watabe, J. Chem. Phys. **93**, 7350 (1990).
[27] V. Hugouvieux, E. Farhi, M. R. Johnson, F. Juranyi, P. Bourges, and W. Kob, Phys. Rev. B **75**, 104208 (2007).
[28] S. Munejiri, T. Masaki, T. Itami, F. Shimojo, and K. Hoshino, Phys. Rev. B **77**, 014206 (2008).
[29] Because of Friedel oscillations, the increase in the particle number around the small hump near 4 Å can be calculated by $\Delta N=4\pi\rho\int_{r_1}^{r_2}(g(r)-g_0(r))r^2dr$, where, as indicated in Fig. 8, r_1 is a distance in front of the small hump and r_2 is that close to the crossing point of $g(r)$ and $g_0(r)$ beyond the small hump. In our calculation, r_1 is set to be 3.24 Å and r_2 is 4.65 Å, and the value of ΔN is almost 0.5.
[30] J. D. Honeycutt and H. C. Andersen, J Phys. Chem. **91**, 4950 (1987). By following the nomenclature in the reference, the ABPs are characterized by four indices. The first index is 1 if the two atoms of a root pair are bonded. The second index represents the number of common neighbors, with each one bonded to the two atoms of the root pair. The third index gives the number of bonds among the common neighbors. These three indices are not sufficient to characterize a diagram uniquely. Therefore, a fourth index is required to specify a unique correspondence between the arrangement of atomic bonds and diagrams.